Supporting information

Reversible Solid State Redox of an Octacyanometallate-Bridged Coordination Polymer by Electrochemical Ion Insertion/extraction

Masashi Okubo[1]*, Koichi Kagesawa[1], Yoshifumi Mizuno[1], Daisuke Asakura[1], Eiji Hosono[1], Tetsuichi Kudo[1], Haoshen Zhou[1]*, Kotaro Fujii[2], Shin-ichi Nishimura[3], Atsuo Yamada[3], Atsushi Okazawa[4], Norimichi Kojima[4]*

[1]*National Institute of Advanced Industrial Science and Technology, Umezono 1-1-1, Tsukuba, Ibaraki 305-8568, Japan*

[2]*Tokyo Institute of Technology, Ookayama 2-12-1, Meguroku, Tokyo 152-8551, Japan*

[3]*Department of Chemical System Engineering, School of Engineering, The University of Tokyo, Hongo 7-3-1, Bunkyo-ku, Tokyo, 113-8656, Japan*

[4]*Graduate School of Arts and Sciences, The University of Tokyo, Komaba 3-8-1, Meguroku, Tokyo 153-8902, Japan*

To whom correspondence should be addressed: m-okubo@aist.go.jp, h.s.zhou@aist.go.jp, cnori@mail.ecc.u-tokyo.ac.jp

Table S1 Rietveld refinement result for MnMo-CCP. The structure is almost isomorphous to $[Mn(H_2O)][Mn(HCOO)_{2/3}(H_2O)_{2/3}]_{3/4}[W(CN)_8]\cdot H_2O$ (T.-W. Wang, *et al.*, *Inorg. Chem.*, (2010) **49**, 7756.). The atomic coordinates and isotropic displacement factor for C4, O1, O1w, O2w, O3w and O4w were not refined, because formic acid and water coordinating to Mn are strongly disordered.

Atom	*g*	*x*	*y*	*z*	B_{eq} / Å^2
Mo	1.0	0.0	0.0	0.13761(8)	1.65(5)
C1	1.0	0.8054(5)	= *x*	0.1577(3)	3.0(1)
C2	0.375	0.787(1)	0.040(2)	0.0786(3)	= B_{eq}(C1)
C3	1.0	0.0	0.0	0.2143(3)	= B_{eq}(C1)
N1	1.0	0.7015(4)	= *x*	0.1679(2)	3.0(1)
N2	0.375	0.6714(8)	0.067(2)	0.0535(3)	= B_{eq}(N1)
N3	1.0	0.0	0.0	0.2536(2)	= B_{eq}(N1)
C4	0.25	0.313	0.313	0.0	1.0
Mn1	0.375	0.5	0.0550(6)	0.0	1.9(1)
Mn2	1.0	0.0	0.0	0.3267(1)	1.37(8)
O1	0.25	0.5	0.695	0.0	1.0
O1w	1.0	0.0	0.0	0.4099	2.0
O2w	0.25	0.5	0.758	0.0	2.0
O3w	0.54(1)	0.5	0.0	0.25	2.0
O4w	0.13(1)	0.5	0.5	0.021(3)	2.0

Space group: *I*4/*mmm*

a = 7.5739(2) Å, *c* = 28.8274(7) Å, *V* = 1653.7(7) Å^3

R_e = 2.34%, R_{wp} = 3.74%, R_p = 2.75%, *S* = 1.60, R_{Bragg} = 1.85%

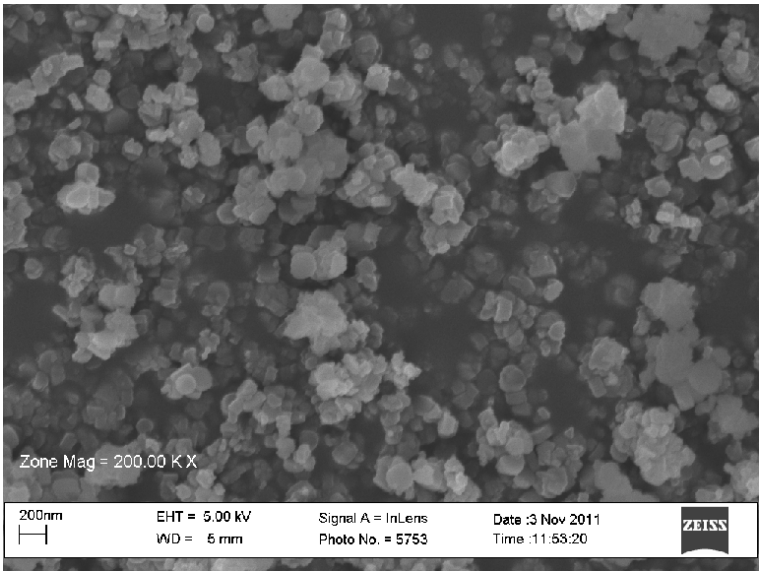

Figure S1 SEM image for MnMo-CCP. The scale bar is 200 nm.

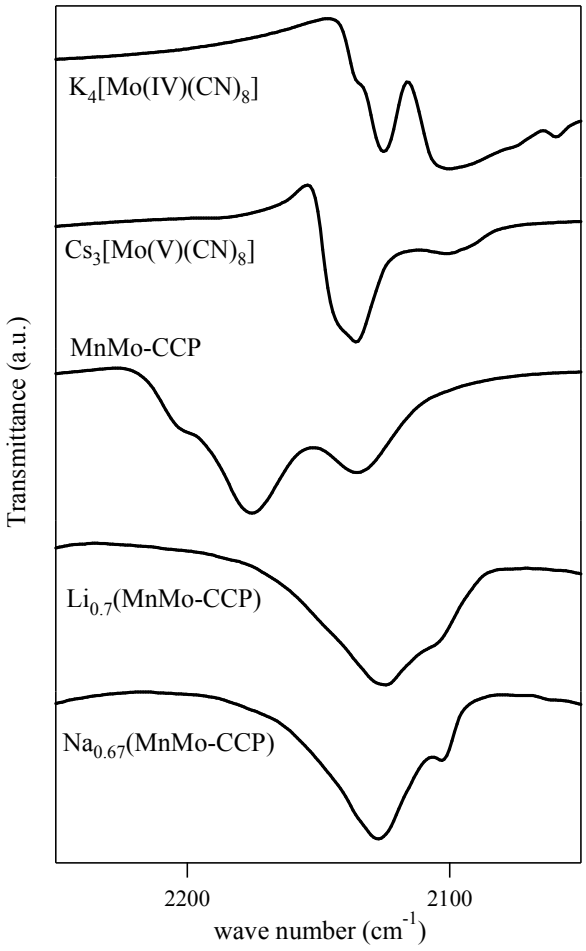

Figure S2 FT-IR spectra for $K_4[Mo(CN)_8]$, $Cs_3[Mo(CN)_8]$, MnMo-CCP, $Li_{0.7}$(MnMo-CCP) and $Na_{0.7}$(MnMo-CCP). Absorption peaks are assigned to the CN stretching modes.

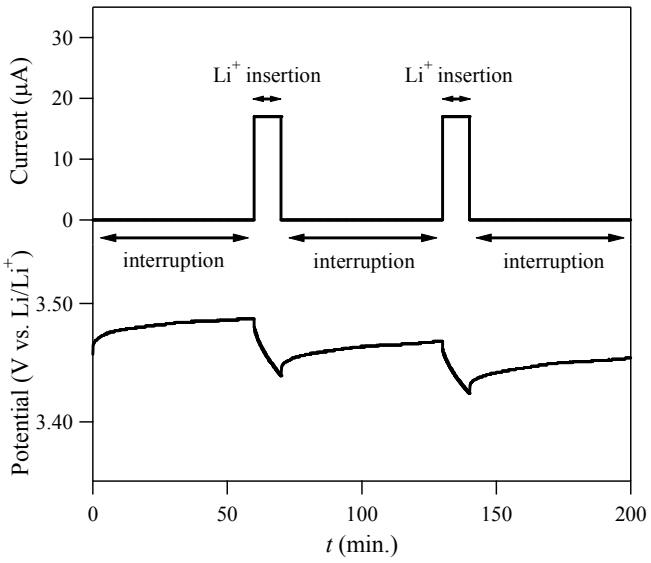

Figure S3 Typical time dependence of the cell voltage and applied current during the insertion of Li-ions by the GITT.

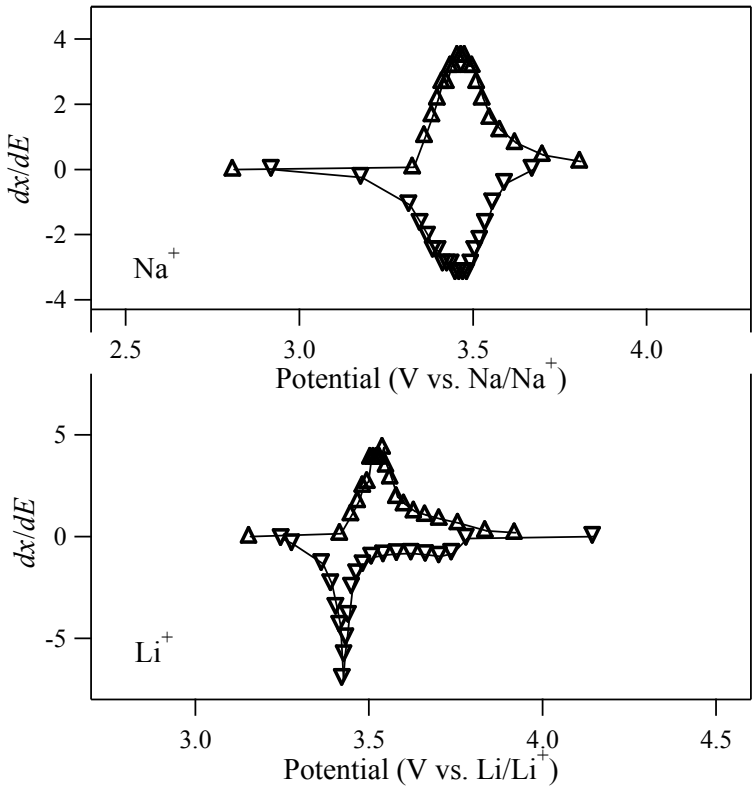

Figure S4 *dx*/*dE* vs. *E* plot of Li_xMnMo-CCP and Na_xMnMo-CCP.

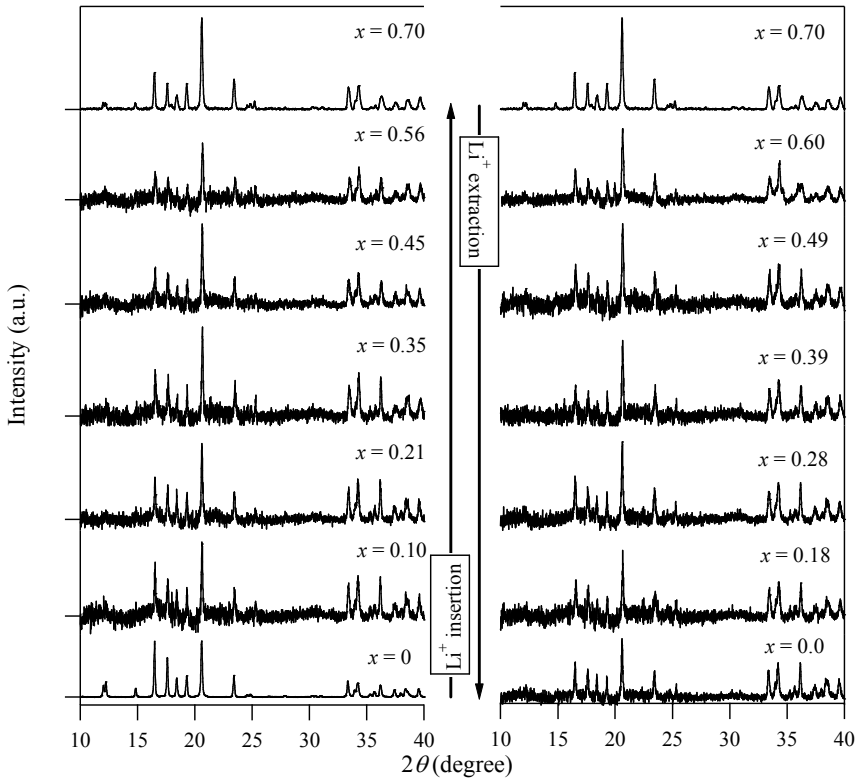

Figure S5 *Ex situ* XRD patterns measured during Li-ion insertion/extraction.

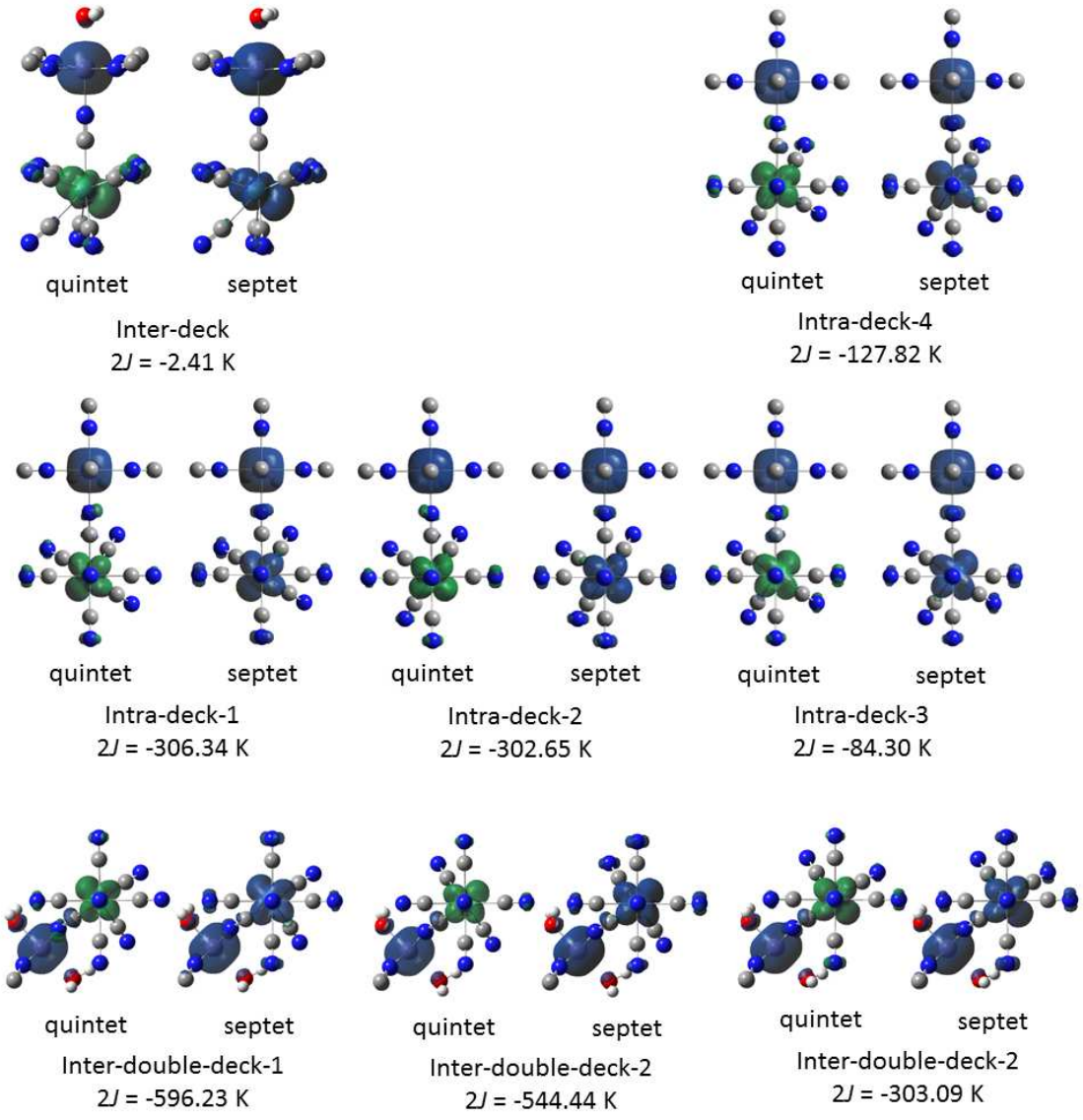

Figure S6 The DFT calculated spin density for all possible Mn-Mo pairs from MnMo-CCP. The blue and green densities correspond to positive and negative spins, respectively.

(a)

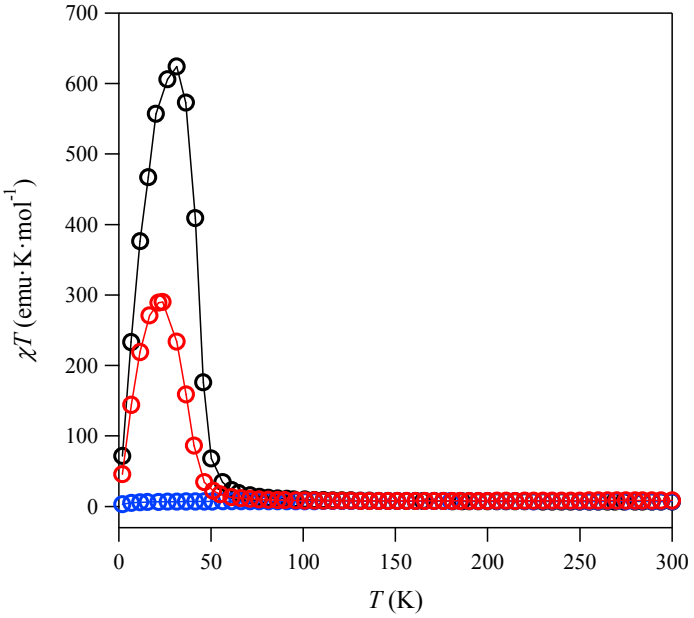

(b)

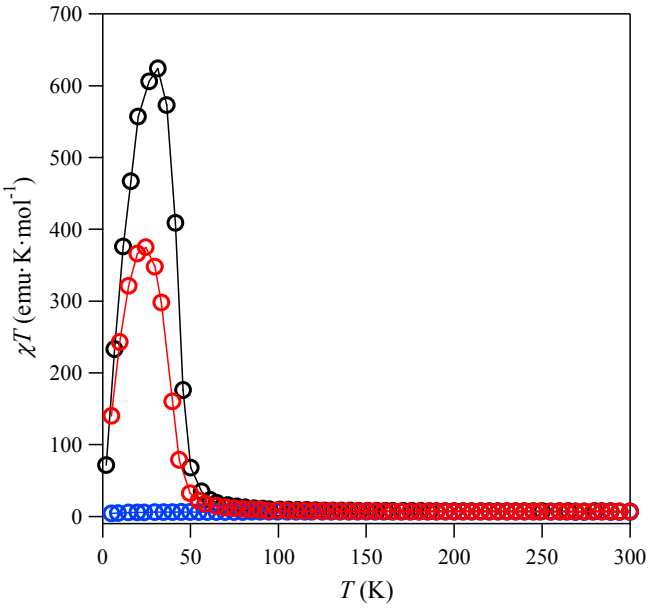

Figure S7 (a) χT vs. T plot of MnMo-CCP (black), $Li_{0.7}$(MnMo-CCP) (blue), and Li_0(MnMo-CCP) (red), (b) χT vs. T plot of MnMo-CCP (black), $Na_{0.67}$(MnMo-CCP) (blue), and Na_0(MnMo-CCP) (red).

(a)

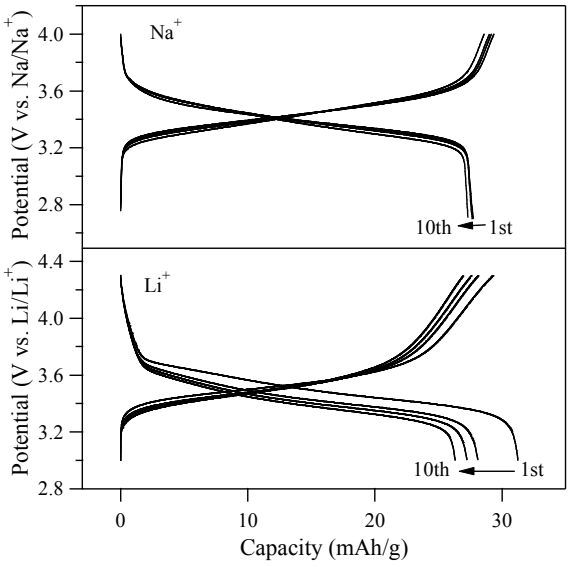

(b)

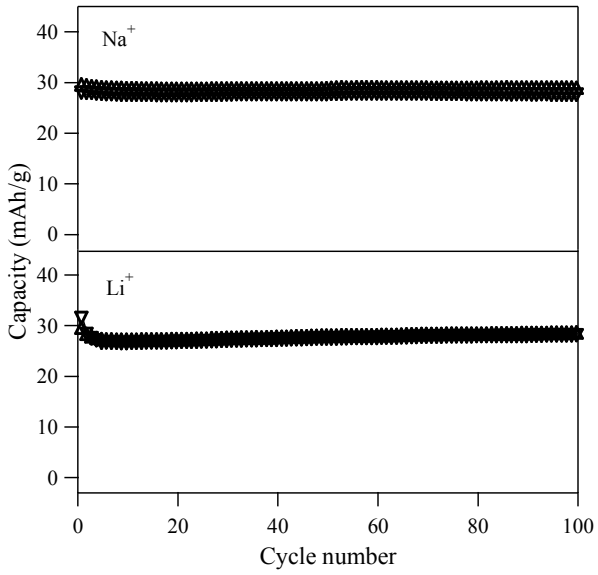

Figure S8 (a) Potential profile during Li-ion and Na-ion insertion/extraction in MnMo-CCP at constant specific current of 10 mA/g. (b) cycle stability of MnMo-CCP for Li-ion and Na-ion insertion/extraction.